Chapter 3

Emission-Line Observations

Peter Tamblyn[1], G. H. Rieke[1], Margaret Murray Hanson[2], L. M. Close[1], D. W. McCarthy, Jr.[1], & M. J. Rieke[1]

[1]Steward Observatory, University of Arizona, Tucson, Arizona 85721

[2]Joint Institute for Laboratory Astrophysics, Campus Box 440, University of Colorado, Boulder, Colorado 80309-0440

Abstract

Br γ and He I 2.058 μm images of the Galactic center reveal that most of the Br γ emission is associated with interstellar gas but that the He I is largely concentrated on individual, luminous stars that therefore must be hot. High-resolution spectra of these stars, emphasizing He I 2.058 μm through Br γ 2.166 μm, are compared with spectra of 98 hot, luminous stars from the literature and new spectra of 43 luminous galactic emission-line stars including late nitrogen-sequence Wolf-Rayet, Luminous Blue Variable, Oe, Of, and ON supergiant stars. Combining our data with other observations from the literature, the He I sources in the central parsec include $\sim$ 5 Ofpe/WN stars and one late-WC star. The inferred luminosity and detection of Mg II emission lines in the spectrum of IRS 16NE make it a likely LBV candidate. However, we find 6 stars with line widths < 500 km/s which defy easy classification, even from the extensive library of comparison spectra we have compiled. Considering the ultraviolet constraints (cf. Serabyn & Lacy 1985; Shields & Ferland 1994) and the large number of peculiar hot stars, either we see this stellar population at a very distinctive moment in its evolution, or the conditions of formation or the evolution of the stars must be significantly altered by the environment in the central parsec.

3.1 Introduction

The center of the Galaxy is in many regards the most easily studied galactic nucleus, despite $\sim$ 30 magnitudes of extinction in the visual. A persistant puzzle is the region's power source. The interstellar gas is excited by $\gtrsim 10^{50}$ ionizing photon s^{-1} with a soft ($T_{\rm eff} \lesssim 35,000\,{\rm K}$) spectral distribution (Lacy *et al.* 1980; Serabyn & Lacy 1985). Although there has been considerable speculation that accretion onto a massive black hole is the dominant energy source, models (Hollywood & Melia 1995) which reproduce the faint infrared flux (Eckart *et al.* 1992; Close, McCarthy, & Melia 1995) indicate that accretion does not dominate the UV. The presence of red supergiants (Lebofsky, Rieke, & Tokunaga 1982) and the "blue" (near-infrared) colors of numerous point sources suggest that a population of young stars powers the region.

Broad He I 2.058 μm emission was detected from the IRS 16 region in the Galactic center (GC) by Hall, Kleinmann, & Scoville (1982). Allen, Hyland, & Hillier (1990) showed that the Br γ source 10″ SW of the dynamical center discovered by Forrest *et al.* (1987) is a strong He I source as well. Their tentative classification of this star, referred to as the AF star, as Ofpe/WN9 was confirmed with high-resolution spectroscopy (Najarro *et al.* 1994). Although it has generally been assumed that the IRS 16 complex could be a group of WR stars with the AF star an outlying example, Chapter 2 used the NIR brightnesses of these stars and a variety of constraints on the integrated properties of the stellar population to show that this would not be consistent with normal stellar evolution. Instead, we suggested that a normal young population consistent with the global constraints would have an ample supply of undetectable late-O main-sequence stars to excite nebular He I emission. Existing He I emission line images (Krabbe *et al.* 1991) can distinguish the AF star and $\sim$ 10 other strong and relatively isolated He I sources from the background. Higher

angular resolution is required to distinguish whether the bright, crowded IRS 16 components are also unusual He I 2.058 μm sources or whether they are the lower temperature supergiants predicted by the evolutionary calculations, with the emission lines originating in the surrounding nebulosity. As reported earlier (Tamblyn & Rieke 1993; Rieke & Rieke 1994), such images indicate the He I does in fact originate in the stars; these data are presented in greater detail here and in the context of their implications for population models of the central cluster.

Further insights to the nature of the hot stellar population can be obtained with spectroscopy, which can be compared with the near-infrared spectra of hot stars elsewhere in the Galaxy to classify the GC stars. We have obtained spectra at a resolution of $\lambda/\Delta\lambda \approx 2500$ of many of the He I sources apparent in our images and those of others. A number of the He I stars appear to be normal late-WN or Ofpe/WN stars. However, many others have relatively narrow lines and cannot be associated with any common stage in normal hot stellar evolution. Both our imaging and spectroscopy therefore indicate either that we see the GC at a very distinctive moment in its evolution or that there is some abnormality in the formation or evolution of massive stars in this region.

In Section 3.2, we describe our high-resolution images of the GC in the He I emission line and complementary Br γ images intended to determine whether the IRS 16 components are individual He I sources. Spectra of many of the He I sources and a large sample of comparison stars are described in Section 3.3. Section 3.4 discusses possible classifications for the population of narrow emission-line stars found in the region. Finally, Section 3.5 summarizes the results from these observations.

3.2 Emission-Line Images

These images test whether the IRS 16 components are hot, He I emission sources, contrary to the predictions of the starburst models with normal stellar evolution (Chapter 2).

3.2.1 Imaging Observations and Reductions

Narrow-band images of the GC south of IRS 7 were obtained in May 1993 and June 1994 at the Steward Observatory Bok (2.3 m) telescope. Atmospheric image degradation is a major concern for imaging the crowded GC field and is exacerbated by the low elevation at transit of the GC as seen from Kitt Peak. Tip-tilt correction for image motion, made possible by FASTTRAC (Close & McCarthy 1994), substantially improved the image quality. FASTTRAC uses a small probe mirror to pick off light from a bright guide star (IRS 7) and send it to an InSb camera read out at ~ 50 Hz to determine the displacement of the stellar image centroid. The displacement is translated into an error signal to drive the tip-tilt telescope secondary to recenter the stellar image. The remainder of the field is imaged to $0.2''$/pixel by the Steward Observatory NICMOS camera (Rieke *et al.* 1993) which has a 256x256 NICMOS3 array used for the longer-integration (120–300 s) science images. These images had a FWHM of 0.8–$1.0''$ in this experiment. A narrow bandpass interference filter was used in a system where the transmission function is tuned by tilting. The tilt of the interference filter was verified by observing a planetary nebula. For He I imaging, the filter transmission has a FWHM of 0.017 μm for a spectral resolution of 120. The Br γ data were measured with a resolution of about 200. Continuum images were obtained by changing the filter tilt to provide transmission with similar spectral resolution displaced slightly from the emission line.

Initial data reduction followed standard procedures. Pixel-to-pixel response variations were removed with dark and flat frames. Images of a blank sky field, taken

after each object image, were median combined in separate groups by night and filter setting. For each GC image, the appropriate blank sky frame was scaled to the same median as the single blank field image taken after the GC image and subtracted. The resulting images are quite flat except for the immediate area around the image of the probe.

Before summing, the images were co-aligned and bad pixel values replaced by interpolation from neighboring pixels. In none of the images were bad pixels located in the IRS 16 environs. In the case of the Br γ pair, the image in the nearby continuum had higher spatial resolution. It was degraded to the resolution of the on-band image by convolution with a Gaussian. The continuum images were scaled and subtracted from the on-band images to create the difference images presented in Figures 3.1*a* and 3.1*c*. In the case of the Br γ pair, there was little ambiguity (6%) about the scaling coefficient as an inappropriate coefficient clearly results in under- or over-subtraction of the stellar images. For the He I pair this uncertainty increases to 10%. In part this is due to the fact that the bulk of the He I emission is from point sources unlike the predominantly diffuse Br γ emission. A few stars (e.g., IRS 9 and IRS 12N) apparently suffer greater extinction or have H_2O absorption and appear over-subtracted when the scaling coefficient is adequate to subtract out the bulk of the stellar images. The over-subtracted stellar residuals were replaced with the local sky value before photometry was performed.

Simulated aperture photometry was performed on the images with the IRAF APPHOT package and compared to published aperture photometry (Wade *et al.* 1987). Our results agree allowing for uncertainty in aperture location. Large simulated apertures were used to estimate the contribution to the line flux from diffuse emission. Even in the difference image, the He I image is crowded and the sources incompletely resolved, so the stellar profile fitting photometry package DAOPHOT

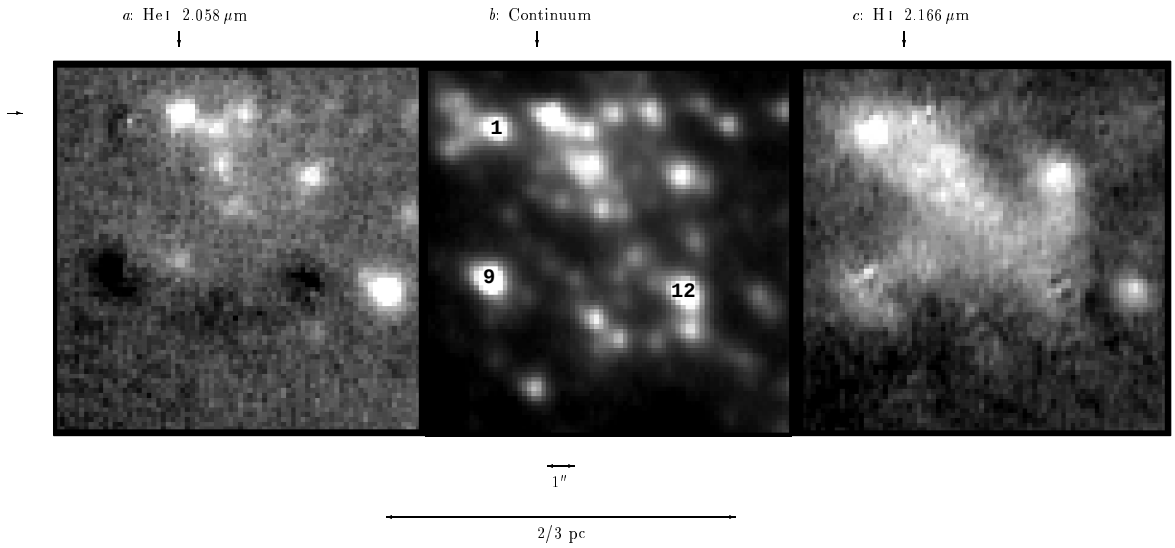

Figure 3.1: Emission-Line Images. The central 0.7 pc south of IRS 7 in *a*: He I 2.058 μm, *b*: nearby continuum, and *c*: H I Br γ. The location of IRS 16C ($17^h42^m29\overset{s}{.}4$ $-28°59'18''$, 1950.0) is indicated by arrows. Sgr A* is 1.1″W and 0.3″S of IRS 16C. IRS 1W, IRS 9, and IRS 12N are labelled for comparison with finding charts such as in Rieke *et al.* (1989). North is to the top and west is to the right.

in its IRAF implementation was used to measure He I fluxes. The two types of photometry could be compared with the isolated AF star. The resulting line fluxes are listed in Table 3.1. Because the He I emission is associated with bright stars, the uncertainty in the scaling coefficient combined with photometric calibration errors is enough to make our measured fluxes and even relative fluxes uncertain. However, the morphology described below is robust to these uncertainties and only sources which were prominent with either extreme of the subtraction coefficient are listed. A handful of fainter sources not associated with prominent stars in the continuum may exist in the region within the uncertainties. However, their number is small and they do not affect the conclusions of this paper.

Table 3.1: Unresolved Line Fluxes in Images

Source	Location	$F_{2.06\,\mu m}$ $10^{-16}\,W\,m^{-2}$	$F_{Br\gamma}$ $10^{-16}\,W\,m^{-2}$
AF (AHH)		2.4	1.8 ± 0.7
GCHe1	1.1″NE of AF	0.8	...
AHH-NW		0.6	...
GCHe2	0.7″N 2.6″W of IRS 9	1.0	0.9 ± 1
GCHe3	$\sim$ 4″S 1″W of IRS 16C	...	...
GCHe4	$\sim$ 4″N 1″W of AF	...	...
IRS 1W		...	2.1 ± 0.4
IRS 13		0.9	2.5 ± 1
IRS 16C+CC		1.8	...
IRS 16NE		1.8	...
IRS 16NW		1.5	...
IRS 29		...	...
GCHe5	$\sim$ 3″SW of IRS 7	...	...
IRS 15		...	...
Integrated		...	35 ± 8

3.2.2 Imaging Results – He I Star Cluster and Sgr A*

The Br γ image in Figure 1*c* has a few bright point sources (IRS 1W, IRS 13, and the AF star) and significant extended emission indicative of gas excited by the ambient radiation field. The morphology is very similar to the Br γ image presented by Lutz, Krabbe, & Genzel (1994) as well as the Br α image of Forrest *et al.* (1987) and radio images of the "mini-spiral" (Morris & Yusef-Zadeh 1987). In contrast, the 2.058 μm image (Figure 1*a*) clearly illustrates that the majority of the He I emission is from point sources, 5 of which are associated with stars prominent in broad-band images (Figure 1*b*) including 4 components of IRS 16. The contrast of He I and Br γ images clearly demonstrates that the He I is not from the surrounding nebula; its association with bright stars requires distinctive luminous stars which may be

difficult to reconcile with population models for the region (Chapter 2).

The observation by Krabbe *et al.* (1991) of He I emission from IRS 9, IRS 11, and IRS 15E is baffling because these objects are known to have CO absorption bands (IRS 9: Rieke, Rieke, & Paul 1989; IRS 11: Sellgren *et al.* 1987; IRS 15: Rieke & Rieke 1988). One of these sources, identified by Krabbe *et al.* (1991) as IRS 9, is in the field imaged in this experiment. With $1''$ resolution, the emission-line source is clearly seen to be a star, near the background confusion limit in the continuum, located $2.6''$ west of IRS 9. Images taken with the same instrument and a CO filter indicate IRS 9, which is a great deal brighter in the near infrared, has significant CO absorption and the previously unnoticed star to the west does not. Hence, this paradox was a result of insufficient spatial resolution blending the spectral diagnostics from a hot–cool source pair. Because it is not obvious how one star could exhibit both features, it seems likely that the remaining CO/He I identifications (IRS 11 and IRS 15E) by Krabbe *et al.* (1991) are also blends of the distinguishing He I feature from a hot star near a significantly cooler, and therefore brighter in the NIR, star with CO absorption.

We note that the He I image suggests the existence of an emission source at the same location (to an accuracy of 1 pixel) as the infrared source detected at H and K by Eckart *et al.* (1993) and at J by Close *et al.* (1995) coincident with the radio location of the black hole candidate Sgr A*. If this result is confirmed, it is likely to be useful in further studies of the nature of this object.

3.3 Spectroscopy

3.3.1 Spectroscopic Observations and Reductions

The confirmation that the He I emission line arises from a number of luminous stars leads to questions about their natures. To address these issues, spectra including

He I (2.058 and 2.112/3 μm), Br γ, and in some cases He II (2.189 μm) were obtained for many of the stars in the image. A large number of luminous galactic emission-line stars were also observed for comparison; many were selected for their high mass-loss rates. These spectra were all obtained with the Steward Observatory near-infrared spectrometer, Fspec, which is based on a NICMOS3 detector. Observations concentrating on the IRS 16 region were obtained on April 28 and 30, 1994 with the MMT, where the Fspec pixel scale is 0.37″, the slit is 1.2″ wide by 32″ long, and the spectral resolution measured from night skylines is 125 km/s. These were supplemented with observations of more isolated stars on June 26 and July 2, 1994 at the Steward Bok (2.3 m) telescope, with a pixel scale of 1.2″, slit 2.4″ by 96″, and measured resolution of 120 km/s. Spectra of the comparison stars listed in Table 3.2 were taken on those same nights and July 15 and 20 with the Bok telescope and in October 1993, April 1994, and October 1994 with the Mt. Bigelow 1.5 m telescope, where the slit width is 3.6″ and the measured resolution is 105 km/s. Observations and data reduction followed standard procedures. Two to three overlapping grating settings were used to cover the wavelength range. Distortion in the spatial axis was determined from the observations of the spectral reference stars which were stepped along the slit. Skylines are strong and common in this spectral region and could be used directly for wavelength calibration. Correction for atmospheric absorption was performed by dividing with a spectral reference observation obtained at the same airmass immediately before or after each object integration. Most of the spectral references were F5-G2V stars for which a correction for photospheric features (see Maiolino, Rieke, & Rieke 1996) was applied. A large number of sources with flat continuum spectra in the 2.058 μm region, not shown in this paper which focuses on the He I feature, confirm that this technique removes atmospheric residuals with a high degree of accuracy. The GC spectra presented have been corrected uniformly

for reddening assuming $A_K = 3.47$ (Rieke *et al.* 1989) and the reddening law of Rieke & Lebofsky (1985); no reddening correction has been applied to any of the spectra of the relatively unobscured comparison stars. No radial velocity corrections have been applied.

For the MMT observations of the GC, the slit was positioned by offsetting from IRS 7. An infrared guiding camera was available for the Bok observations, allowing precise placement of the slit. Although the position of the slit on the field can be determined fairly accurately by comparison of the intensity along the spatial axis with a high-resolution continuum image, many of the GC sources described here are not dominant continuum sources. With slit widths 1.2–2.4″ and pixel scales 0.4–1.2″/pixel, it is not always possible to determine the location of an emission source uniquely. In a few cases (e.g., AHH-NW), multiple slit positions allow an accurate determination of the source location. More generally, a best estimate was made from the source position on the spatial axis and the source was assumed to be the nearest He I source detected in our He I image or that of Krabbe *et al.* (1991) for sources north of IRS 16.

The slit angle on the sky was varied for optimal coverage of the most interesting sources. A nearby, heavily obscured region was used to monitor the sky level because of the extended nature of the GC stellar distribution. There is significant spatial structure in the background which is generally confused at the spatial resolution of these data, especially in the Br γ line. To minimize contamination, one-dimensional spectra were extracted using simulated apertures 2 pixels wide. It is noted in the text when subtraction of the stellar and nebular background is likely to have distorted the spectral features. The continuum level is generally significantly contaminated by cool stars; hence, the equivalent widths of the emission features are very uncertain. Similarly, because many of the sources were not centered on the slit, line fluxes can

Table 3.2: Comparison Star Features

Source	Type	He I 2.06	C IV 2.08	He I 2.11	N III 2.12	Mg II 2.14	H I... 2.17	He II 2.19
HD 50896 (WR 6)	WN5	we		e	?		se	
HD 192163 (WR 136)	WN6	a		e			e	e
HD 191765 (WR 134)	WN6	a		wa			se	e
Roberts 89 (WR 120)	WN7	e^P		e			se	e
HD 177230 (WR 123)	WN8	se^P		se^P			se	e
AS 268 (WR 105)	WN8	se^P		e			se	we
AS 306 (WR 116)	WN8	se^P		se			se	we
HD 313846 (WR 108)	WN9	a	e	a			e	a
NaSt 1 (WR 122)	WN10	se		se			e	e
P Cyg	B2pe (LBV)	se^P		e		e	se	
HD 160529 [SN]	A3Iae (LBV)							NA
HD 15570	O4If+	wa	e		e	NA	e	wa
HD 14947	O5.5f	wa	e		e	NA	e	wa
HD 15558	O5.5III(f)		e		e	NA	a	
HD 190864	O6.5III(f)	a	e		e	NA	a	a
HD 36861	O8III(f)	a	we	a	e	NA	a	
HD 46150	O5V((f))				e	NA	a	wa
HD 15629	O5V((f))	wa	e		e	NA	a	wa
HD 229232	O5e				e		e	a
HD 39680	O6:pe	se		e		we	e	NA
HD 194334	O7.5Ve	a		a	e		e	a
HD 225160	O8e	a					a	
MWC 627	O8e	e^D					se	NA
HD 60848	O8V:pevar	e^D		NA	NA	NA	NA	NA
X Per	O9pe	e^D				NA	e	
SAO 20924	B0III/O9e			NA	NA	NA	NA	NA
HD 185859	B0.5Iae	we?		a			a	NA
HD 2905	B1Iae	e		a			a	NA
HD 207329	B1.5Ib:e	e		a			e	
HD 41117	B2Iaevar	e		a			a	NA
HD 206267	O6V				e	NA	a	
HD 199579	O6V	a		wa		NA	a	wa
V645 Cyg [SN]	O7			NA	NA	NA	NA	NA
HD 210809	O9Ib	a		a		NA		wa
HD 193322	O9V((n))	wa		a		NA	a	
HD 214680	O9V	wa		a		NA	a	
HD 209975	O9.5Ib	a		a		NA	a	
BD+36 4063 [R]	ON9.7Ia	e		a			e	
HD 191781 [R]	ON9.7Ib	we		a			we	
BD+59 2786	B0III			wa			a	NA
HD 38771	B0Iab:	e		a			a	NA
HD 37128	B0Iab:			a			a	NA
HD 14143	B2Ia	e		a			a	NA
HD 183261	B3II						a	NA
HD 14134	B3Ia			NA	NA	NA	NA	NA

e: emission a: absorption w: weak s: strong NA: not available

[SN] Relatively poor signal-to-noise. Weak features undetectable.

[R] Only R=500 spectrum available.

[P] P Cygni profile.

[D] Disk signature.

Table 3.3: Properties of Galactic Center Sources

Source	$W_{2.06\,\mu m}$ μm	FWHM km/s	$W_{2.112\,\mu m}$ μm
GCHe4	0.0035	1200	0.0006
AHH-NW	0.0046	1000	0.0020
IRS 15	0.0022	1000	...
GCHe5	0.0336	900	0.0054
IRS 13	0.0025	480	0.0009
IRS 16NW	0.0010	360	−0.0002
IRS 29	0.0006	320	...
GCHe2	0.0010	250	...
IRS 16NE	0.0009	180	−0.0001
GCHe3	0.0008	130	...
IRS 1	0.0004	< 120	...

be more accurately determined from the images.

3.3.2 Spectroscopy Results – Stellar Classifications

Figures 3.2 and 3.4 show the spectra of the GC sources observed. Table 3.3 lists measured properties of some of the prominent spectral features seen in the GC sources. The [Fe III] (2.145 and 2.218 μm) and H_2 (2.122 μm) lines are background features (cf. Lutz *et al.* 1994). Table 3.2 lists the comparison stars observed and Figures 3.3 and 3.5 show the spectra of the most relevant. The spectrum of NaSt 1 (WR122 in van der Hucht *et al.* 1981) has been truncated for presentation: the 2.058 μm line continues to 33 times the continuum level. Outside the late-WN sample, strong emission at 2.058 μm is clearly a rarity in the comparison sample despite preferential selection of spectral types most likely to exhibit this line. This is consistent with the expectation that this line is only strong in enriched stars undergoing strong mass loss and extends the result of Hanson & Conti (1994) in which only 1 of 19 O4–B3 stars had strong emission in this line.

Wide Emission Lines — Ofpe/WN9 Candidates

Four of the GC sources listed in Table 3.3 (GCHe4, AHH-NW, IRS 15, and GCHe5) have broad emission lines. The former two are seen in different spectra at close to the same location and may actually be a single source. The differences in the 2.058 μm profiles may be due to the subtraction of slightly contaminated backgrounds.

In regions crowded with emission sources, superposition of velocity-displaced profiles can mimic the appearance of a broad emission line (as seen in the low spatial resolution observations of Hall *et al.* 1982). However, these four are probably signatures of fast winds because these sources are not in the crowded IRS 16 region. P Cygni profiles seen in 3 of the spectra, most prominently for the source GCHe4, confirm this. The He I doublet at 2.112/3 is also seen in these sources. Their K magnitudes range from just above the background, $m_K \sim 12$, up to $m_K = 9.5$ (if the dominant continuum source in IRS 15 is the emission source). With correction for extinction, this corresponds to M_Ks of ~ -6 to -8.6.

These sources appear quite similar to the AF star (Allen *et al.* 1990; Najarro *et al.* 1994; Libonate *et al.* 1995) and to the later WN comparison stars, as WR116 in Figure 3.2 illustrates. Classification of late WN and extreme Ofpe stars is subject to debate (cf. Crowther, Hillier, & Smith 1995), made worse in this case by the unavailibility of optical or UV spectra of the GC sources. The comparison WN stars (also Figure 3.3) illustrate that the primary NIR criterion used to date, the He II 2.189 μm feature, is often relatively weak in the WN8–10 classes and the absence of this feature should not exclude a WN classification. It should be noted that although HDE 313846 (WR108) is the only Galactic WN9, it is considered a poor prototype of the class (Walborn 1982), and NaSt1 (WR122) has been compared to B[e] stars (Crowther *et al.* 1995). Until a meaningful differentiation of the late-WN and Ofpe classes in the NIR is identified, we will follow Allen *et al.* (1990)'s example and

classify these GC stars as Ofpe/WN9s with the note that they appear more in step with the WN progression than the Of or Oe examples in our comparison suite. The near-infrared brightnesses of these stars are in agreement with this classification.

Narrow Line Sources

Unlike the stars discussed above, seven sources have relatively narrow (< 500 km/s) 2.058 μm emission features which distinguish them from WRs and Ofpe/WN9s, including the AF star and the WC9 in the GC discovered by Blum, Sellgren, & DePoy (1995b). This distinction was first pointed out for IRS 13 and IRS 16NE by Libonate *et al.* (1995), who suggest an identification as LBV stars.

IRS 16NE: This is one of the brighter sources in the region and also one of the strongest He I sources, hence its spectrum is only lightly contaminated by the nearby stars. As Figure 3.4 and Table 3.3 show, this source has narrow (FWHM 160 km/s) 2.058 μm emission with P Cygni absorption. The 2.112/3 μm He I feature is in absorption. This source is fairly close to the strong Br γ source IRS 1W, so these spectral data do not allow us to determine if it has Br γ emission, but even before any background correction the He I 2.058 μm/Br γ flux ratio is 1.4. The Br γ images (this paper; Lutz *et al.* 1994) do not have a point source at this position bright enough to stand out against the nebular emission, but the Br α image of Forrest *et al.* (1987) does. Hence, IRS 16NE does still have hydrogen in its envelope. The detection of Mg II (2.137 and 2.144 μm) in the spectrum of IRS 16NE distinguishes it from all of the sources in our comparison sample except P Cyg (LBV) and HD 39680 (O6:pe). This doublet, also seen in other LBVs, is excited by fluorescence when Ly β is velocity broadened (McGregor, Hyland, & Hillier 1988b). The roughly equal fluxes seen in these lines in IRS 16NE and P Cyg argues for a fast stellar wind as the fluorescence requires doppler shifts of 73 and 116 km/s to populate the upper states. This is

confirmed by the measured widths of the He I 2.058 μm (less contaminated than Br γ) features of 160 and 175 km/s in IRS 16NE and P Cyg respectively. IRS 16NE is also one of the brighter infrared sources with an implied luminosity $\gtrsim 10^6 L_\odot$ (for $T_{\rm eff} \gtrsim 15,000$ K). These two characteristics in addition to the strong He I emission make it the most likely LBV candidate in the GC.

IRS 13: Our spectrum of IRS 13 illustrates the same, narrow emission features of He I, Br γ, and [Fe III] seen by Libonate *et al.* (1995) in this wavelength range. The [Fe III] features (2.145 and 2.218 μm) are nebular (Lutz *et al.* 1994). The broad base to the other emission lines is likely due to contamination from the large gas velocities in this region. The narrow line component (FWHM 175 km/s) peaks at the continuum location of IRS 13. This source has been resolved (Eckart *et al.* 1993) and the equivalent widths of the emission lines are certainly substantially diluted. Again, the relatively narrow lines distinguish this source from the AF star (emphasized by Libonate *et al.* 1995) and the broad-line sources discussed above. The relative strength of the He I 2.112/3 μm doublet and absence of Mg II features makes the comparison to P Cyg less compelling than for IRS 16NE. Other possible classifications will be discussed below.

IRS 16NW: Although the apparent Br γ absorption in this spectrum is just an artifact of background subtraction, the P Cygni signature in the He I line is real. The emission profile is certainly distorted by the background but is readily distinguishable from the wide lines discussed in the previous section: FWHM of the He I feature before and after background subtraction is 460 km/s and 360 km/s, respectively. There is a marginal emission feature at He II 2.189 μm, but with He I 2.112 μm in absorption, it seems unlikely that this is real.

IRS 1: Spectrally unresolved 2.058 μm emission weakly peaks in the IRS 1 region. We see the feature in spectra taken with both the MMT and Bok telescopes, but

no emission is evident in our 2.058 μm image. Emission with FWHM 540 km/s was reported by Krabbe *et al.* (1991), but only weak, diffuse emission was seen by Libonate *et al.* (1995) who discuss the possibility that the GC sources may have variable emission features. Alternatively, this source may not be detected in our image because the imaging is not as sensitive to weak emission as is the spectroscopy, and Libonate *et al.* (1995)'s coarser pixel scale may have made differentiation between the weak peak and surrounding nebulosity impossible. It is not clear why a much wider emission line was reported by Krabbe *et al.* (1991). IRS 1W is a bright red source with a blue core (Rieke *et al.* 1989) which has even been detected at 0.95 μm (Henry, DePoy, & Becklin 1984), so our data may apply to a hot star buried in the thermally reradiating dust. However, the level of emission and He I/Br γ ratio are also consistent with nebular emission from material of approximately solar composition and the lack of an obvious P Cygni feature makes identification with a stellar wind source uncertain. The spectrum presented has been background subtracted; a velocity displacement of the background Br γ line results in the peculiar Br γ profile.

IRS 29: IRS 29 is near the 10 μm source IRS 3, suggesting that this narrow emission feature may be similar to IRS 1. However, there is clear P Cyg absorption on the 2.058 μm feature. This spectrum has not been background subtracted and the absorption feature is well removed from the 2.0558 μm skyline, so this feature is not a false absorption from over-subtraction. Hence, this line probably does originate in a stellar wind. The thin peak of the He I line has a FWHM of 160 km/s. Comparison with a nearby spectrum along the slit shows that the more extended nebular component is responsible for the broader base.

GCHe2: As mentioned in Section 3.2, this is probably the source detected by Krabbe *et al.* (1991) which they identified with the red supergiant to the east, IRS 9. An emission peak 600 km/s to the blue of H I Br γ arising from blended He I (7-4) tran-

sitions (which span 2.158–2.165 μm, Najarro *et al.* 1994) is clearly distinguishable from H I Br γ; this He I emission feature is also distinguishable from Br γ in the spectrum of P Cyg and quite prominently in that of NaSt1 (WR122). This spectrum has not been background subtracted, and part of the 190 km/s FWHM and at least half of the flux is from the background. An extraction farther to the east has a similar but extended 2.058 μm feature displaced by $\sim$ 150 km/s; only emission from GCHe3 is seen to the west.

GCHe3: The location of this source is relatively poorly determined from these data. It is seen in two nearly perpendicular spectra, but the nearest source to the intersection in the 2.058 μm image is 1″ to the northeast. Both spectra were taken with the 2.4″ slit, so such a displacement is possible and we have assumed this identification. No background subtraction has been applied because other emission sources (GCHe2 and IRS 13) dominate nearby positions on the slit, but the main, unresolved peak of the He I feature is localized. No P Cyg absorption is seen. A feature at 2.143 μm due to Mg II 2.144 μm or [Fe III] 2.145 μm is seen. The [Fe III] identification is much more likely as this source is within the region bright in [Fe III] 2.218 μm (Lutz *et al.* 1994) and the 2.137 μm feature of Mg II is not seen.

Comparison Sample

In addition to the WN series discussed above, comparison stars observed for this project include a large variety of other spectral types as delineated in Table 3.2. Also included are two noteworthy ONIa stars observed on September 24, 1994 at R=500 with CRSP on the KPNO 1.3 m for another project. A few of the comparison stars have weak 2.058 μm features, but only P Cyg and subsets of the Oe/Be and ON stars are strong emitters. We have found no common class of star similar to the GC narrow-line stars. The literature already has a number of high-quality NIR spectra

of late-WC stars (Eenens, Williams, & Wade 1991; Eenens & Williams 1994); some WC9 stars (WR70, WR92, and WR103) have strong 2.058 μm emission lines, similar to the GC star discovered by Blum *et al.* (1995b). Our comparison sample does not duplicate this work nor does it include any Ofpe/WN9 stars. A number of these stars in the Magellenic Clouds also exhibit prominent He I 2.058 μm emission (McGregor, Hillier, & Hyland 1988a). The example in the GC, the AF star, has significantly wider emission lines than the majority of the GC He I stars which are likely a different type of star.

3.4 Discussion — The Collection of Stars

In the preceding sections, we have identified 3–4 Ofpe/WN9 candidates in the GC in addition to the AF star and 7 sources of narrow He I 2.058 μm emission. Table 3.4 lists these and the other stars in the region with published spectroscopy (Najarro *et al.* 1994; Libonate *et al.* 1995; Blum *et al.* 1995b). One of the narrow-line sources (IRS 16NE) is a likely LBV candidate and another (IRS 1) may be non-stellar, but the remaining 5–9 narrow-line stars pose a challenge to interpretation of the cluster of He I stars. Prior to this spectroscopic study, the assumption that the He I sources are WR-like stars (e.g., Krabbe *et al.* 1991) was difficult to reconcile with normal stellar evolution (Chapter 2). Recognition that some of these sources are readily distinguishable from WR and Ofpe/WN9 stars on the basis of line widths (Libonate *et al.* 1995) led to an appeal to less common stellar types (LBV). However, the finding that most of the GC hot stars are of this latter type, with narrow emission lines, demands comparison with a more common stellar class. Data in the literature indicate that the latest WC classes and Ofpe/WN9 stars have prominent but wider emission lines. The comparison sample indicates the same for late-WN stars and that LBV, Oe/Be, and ON supergiants are the only other classes of stars likely to

Table 3.4: Hot Stars with Published Spectroscopy

Name	Offset from IRS 16C	Spectral Type	m_K	Notes
Blum-WC9	$-10.7''$, $-6.0''$	WC9	10.6	C III, C IV
GCHe4	-9, -4	Ofpe/WN9	...	
AHH-NW	-9.4, -3.8	Ofpe/WN9	11.8	
AF	-8.2, -7.5	Ofpe/WN9	11.1	2 He I stars
IRS 6E-N	-6.3, $+1$	narrow	10.8	
GCHe5	-2, $+2$	Ofpe/WN9	...	
IRS 13	-4.7, -2.0	narrow	9.1	
IRS 34?	-4.5, $+1$	narrow	...	
IRS 29	-3.2, $+1.0$	narrow	...	
IRS 15	-2, $+11$	Ofpe/WN9	9.3	
IRS 16NW	-1.4, $+0.8$	narrow	10.1	
GCHe3	-1, -4	narrow	...	
IRS 16SW?	-0.1, -2	...	...	
IRS 16C+CC	0, 0	narrow	9.8+10.6	
IRS 16NE	$+1.3$, $+0.7$	LBV?, narrow	8.8	Mg II
GCHe2	$+1.4$, -6.0	narrow	...	
IRS 1?	$+4$, $+0.2$	narrow	9.3	weak He I 2.058

have prominent emission in this line.

3.4.1 Problems with LBV Classification

Is it reasonable to suppose that all of the GC narrow-line $2.058\,\mu$m sources are LBVs with IRS 16NE the most striking example? This seems unlikely for two reasons. First, the LBV phase of stellar evolution is very brief and experienced only by stars within a limited range of masses; there are only 5–9 known examples in the Galaxy (Humphreys & Davidson 1994). Hence, it is quite unlikely that a significant number inhabit this sub-parsec region. This argument is made stronger by considering that the $2.058\,\mu$m emission line used to pick out these stars should be inefficient at identifying LBV candidates. As HD 160529 in our comparison sample

indicates, many LBVs are not hot enough to be prominent sources of 2.058 μm emission. This implies that there should be many more LBVs in the region than those identified through this emission line. This can be directly ruled out: although main-sequence O stars would be lost in the confusion of the region, all of the LBVs listed in Table 4 of Humphreys & Davidson (1994) are luminous enough that they would be identified as blue sources in color maps (Rieke *et al.* 1989; DePoy & Sharp 1991; Eckart *et al.* 1993) of the region. However, almost all of the blue sources in these maps have been accounted for as He I stars. Second, the bulk of the He I sources are a factor of a few fainter in the near infrared than IRS 16NE, implying that they are either less luminous or hotter. The lowest luminosity LBV listed in Humphreys & Davidson (1994) Table 4 (R71) would have $m_K \approx 10.4$ if placed at the GC. AE And would be fainter, with $m_K \approx 11.6$, despite being more luminous because it is hotter than R71. In comparison, most of the GC narrow-line sources are fainter than would be expected for typical LBVs. For these two reasons, it is implausible that the bulk of the GC He I sources are LBVs.

3.4.2 A Collection of Oe Stars?

Although the one source in Hanson & Conti (1994) which exhibits significant He I 2.058 μm emission is the O7.5IIIe star, HD 155806, there are two arguments against the GC stars being of Oe/Be type. We have 8 Oe and 4 early-Be stars in our comparison sample including 3 selected for 2.058 μm emission seen in lower resolution spectra (Hanson *et al.* 1996). Even among this sample, only 6 share the trait of prominent 2.058 μm emission. As discussed above, limits on the number of blue stars without He I emission make problematic any identification with a blue stellar class in which this emission is not the norm. The emission-line profiles present another difficulty. Oe stars have high mass-loss rates and a disk or asymmetric mass-loss signature, similar to Be stars. As HD 2905 and HD 41117 illustrate, the emission

features can be fairly narrow and apparently Gaussian in profile, but the majority have obviously wider emission profiles, frequently including disk signatures not seen in the GC sources. Presumably this difference is a projection effect: HD 2905 and HD 41117 may be seen relatively face on to their mass-loss disks or asymmetric winds such that the velocity structures are not evident at this resolution. It is possible that some or all of the GC narrow-line sources are also face-on Oe stars, but it is not obvious why they would have a preferred orientation such that we would not detect any disk signatures in this sample of 5 (allowing for the possibilities that IRS 16NE is an LBV and that IRS 1's He I emission is nebular). Hence, although the relative line strengths are consistent with a minority of Oe stars, the line widths are not consistent given reasonable luck on projection angles for the disks.

3.4.3 ON Supergiant Stars

ON stars are a minority population of otherwise normal, H-burning O stars with enhanced surface abundances of CNO cycle products (Conti, private communication; Smith & Howarth 1994). BD+36 4063 (ON9.7Ia) and HD 191781 (ON9.7Ib) have emission at He I 2.058 μm and Br γ. A low-resolution spectrum of the former is included in Figure 3.5. Its equivalent width in the He I feature is comparable to the B1Ie stars in the comparison suite and the weaker GC narrow-line stars. HD 191781 has weak emission features, but if BD+36 4063 is more typical of the class, late-ON supergiants are an intriguing possible classification for the fainter GC He I stars. They have an appropriate brightness and are not expected to have the disk profiles exhibited by the Oe stars. As a minority population, they cannot explain the bright He I stars given the absence of a large number of equally bright blue sources without the He I feature as argued above. However, the contribution to the background from normal O stars remains largely unconstrained, and the sources such as IRS 29 may represent a subset with the ON characteristic.

3.4.4 Comparison with Nearby Populations

The cluster of hot stars in the central parsec can also be contrasted to the young, hot stars found within 40 pc of the GC. Cotera *et al.* (1996) have published infrared spectra of 17 hot emission-line stars which are found in this larger region. Unfortunately, these $\lambda/\Delta\lambda = 250$ spectra cannot distinguish the widths of the emission lines, but only three have prominent He I 2.058 μm emission. The population in the central parsec is considerably more biased towards stars with strong 2.058 μm emission. This indicates that the GC stellar cluster is of a very distinctive age or that conditions of formation or evolution are significantly different from those even just outside this region. For example, explanations for the GC population which rely on metallicity seem unlikely. The uniquely high stellar densities, location at the dynamical center, or possible presence of a central massive object may influence star formation or evolution in the central parsec and distinguish this region from other star formation regions nearby.

In the presence of so many apparently evolved, luminous stars, another surprising aspect of this population is the absence of earlier WR stars. At first appraisal, this may appear to be a selection effect because the hot stars have been identified through one emission line. As the sample of WN stars in Figure 3.3 illustrate, this 2.058 μm line is strongly in emission only in WN8 and later WNs. Also, earlier WRs are less luminous than LBVs and would be faint enough to escape detection as blue continuum sources. However, the He II features are strong in the earlier WN stars, and Werner *et al.* (1991) put a limit $W_{\mathrm{He\,II}\,3.09\,\mu\mathrm{m}} \lesssim 0.05\,\mu$m on 35 continuum sources in the central 20″. Also, the UV radiation field is inconsistent with a significant number of luminous stars hotter than $\sim 35,000$ K (Serabyn & Lacy 1985; Shields & Ferland 1994). Hence, there is not a large population of undetected WR stars of earlier type. This presents a significant constraint on starburst models of this

population.

Similarly, the He I emission line should be inefficient at detecting WC stars. Although a subset of late-WC stars exhibit strong 2.058 μm emission (Eenens & Williams 1994), of which the Blum *et al.* (1995) WC9 star is an example, most late-WC stars do not. However, the C IV triplet at 2.08 μm is usually very strong in these stars. Images of the region were also obtained in this emission feature using the same instrument as described in Section 3.2 in June 1994 with a spectral resolution of 150. They do not show any point emission sources above a 3σ detection threshold of 1.4×10^{-16} Wm^{-2}, indicating there is not a large population of undetected late-WC stars. This is apparently at odds with the Galactic trend with radius which would predict a high WC/WN ratio in the GC. However, this trend applies to constant star formation rate populations rather than burst populations for which age can be a dominant factor (Maeder & Conti 1994). Nonetheless, the observed dearth of WC stars is another important constraint on models of this population especially given the larger number of late-WN or Ofpe/WN9 stars found in this study.

3.4.5 Ultraviolet Contributions

Despite the identification of many luminous emission-line stars, it is still not clear that they dominate the UV field. The Ofpe/WN9-like stars are not luminous enough; IRS 16NE is quite luminous, but probably cooler. The He I 2.112 μm emission feature in IRS 13 suggests it is one of the hotter stars, but the brightness of the emission component of this resolved source is unknown. Hence, although the He I 2.058 μm flux is clearly dominated by these stars, the region's ionization still might be produced by a large number of undetected main-seqence O stars. These stars would be individually too faint to be detected in the near-infrared continuum, but in aggregate dominate the UV.

3.5 Summary

Emission-line images with $1''$ resolution of the southern portion of the GC field indicate the following:

1. The Br γ line flux is predominantly from diffuse emission indicative of gas ionized by the ambient radiation field. There are three unresolved point sources: IRS 1W, IRS 13, and the Ofpe/WN9 AF star.

2. At least one of the sources reported to have He I emission and CO absorption is resolved into a hot/cool stellar pair.

3. The He I line flux is predominantly from nine or more point sources which dominate over the diffuse contribution. This result argues against the possibility that these sources are normal stars undergoing normal evolution.

4. The unambiguous association of the He I emission with stellar sources rather than with diffuse nebulosity, which likely would be subject to significant non-gravitational forces, indicates that these stars are useful dynamical test particles. Emission-line velocities for these early-type stars can provide a new dynamical constraint in the crucial central region where other probes fail (see Haller *et al.* 1996).

New 2 μm spectral observations of the GC He I stars and a sample of luminous emission-line comparison stars lead to these conclusions:

1. Four new Ofpe/WN9 (or late-WN) stars are identified in the central parsec.

2. We confirm that IRS 13 has relatively narrow emission lines including a He I 2.112/3 feature (Libonate *et al.* 1995).

3. IRS 16NE has very unusual Mg II features at 2.137 and 2.144 μm. These, its line widths, and its brightness make it a likely LBV candidate.

4. We find a number of GC sources with narrow 2.058 μm emission features which defy easy classification. He I 2.058 μm emission is a common feature of Oe stars, but the profile is frequently distinguishably different from the profiles exhibited by the GC narrow-line stars. ONIa is a possible classification for the fainter examples.

5. It is not obvious that these stars dominate the region's ionization.

These spectra emphasize the importance of spectral resolution in studying this population as the line widths and profiles have proven to be important distinguishing features. High spatial resolution is also required to avoid confusion even in the emission lines in the central region which is crowded with emission-line stars.

A current census of the known hot stars at the GC includes a WC9 star, 5 Ofpe/WN9s, 1 LBV candidate, and at least 5 additional stars of unknown type with narrow He I emission lines. Although it has been argued that the small number of WR and Ofpe/WN9 stars observed is consistent with a normal starburst (Schaerer 1994), an explanation must now be found for this extraordinary concentration of luminous stars, many of which are clearly very rare types.

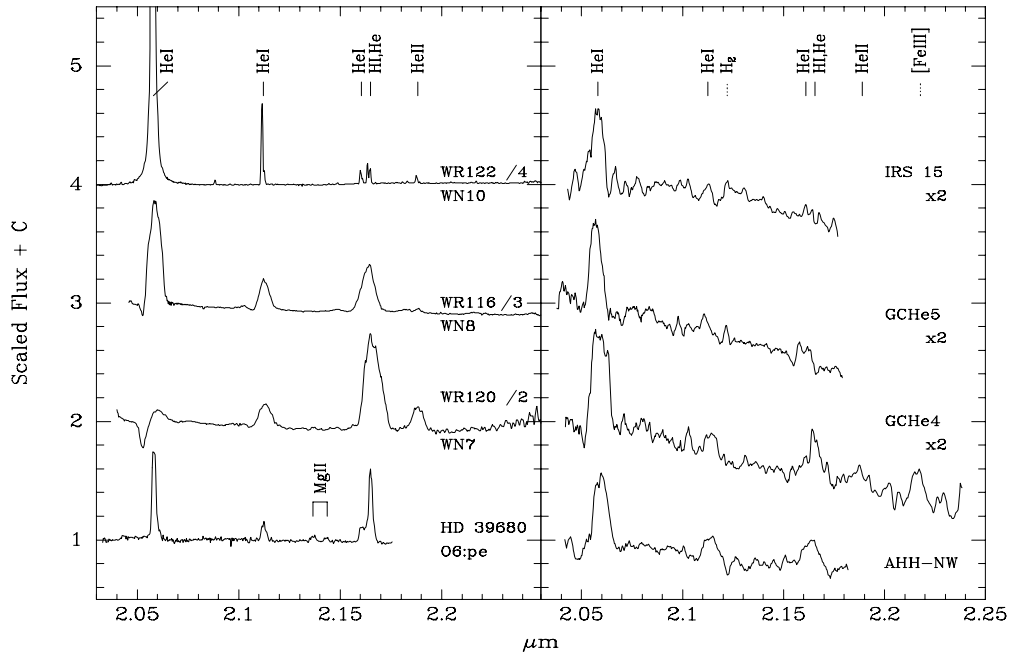

Figure 3.2: Candidate Ofpe/WN9 or Late-WN Stars with Selected Comparison Spectra. The comparison spectra illustrate that the 2.058/2.112 μm ratios and line widths are consistent with a late-WN classification. As Figure 3.5 illustrates, HD 39680 is the closest match among the non-WN stars in the comparison sample. The reader should also compare to the spectrum of the AF star (Najarro *et al.* 1994; Libonate *et al.* 1995), the Ofpe/WN9 stars in McGregor *et al.* (1988b), the GC WC9 star in Blum *et al.* 1995b, and the WC9 stars WR92 and WR103 in Eenens & Williams (1994) (in contrast to WR88). After normalization to the continuum level, these spectra have been scaled as indicated and shifted for convenient presentation. The GC spectra have had approximate background correction applied, dereddening for $A_K = 3.47$, and some smoothing. Br γ is likely to be severely distorted in all cases. Subtraction of background H_2 2.122 μm and H I 2.166 μm is responsible for the peculiar profiles of AHH-NW. [Fe III] 2.218 μm in GCHe4 is a residual nebular feature.

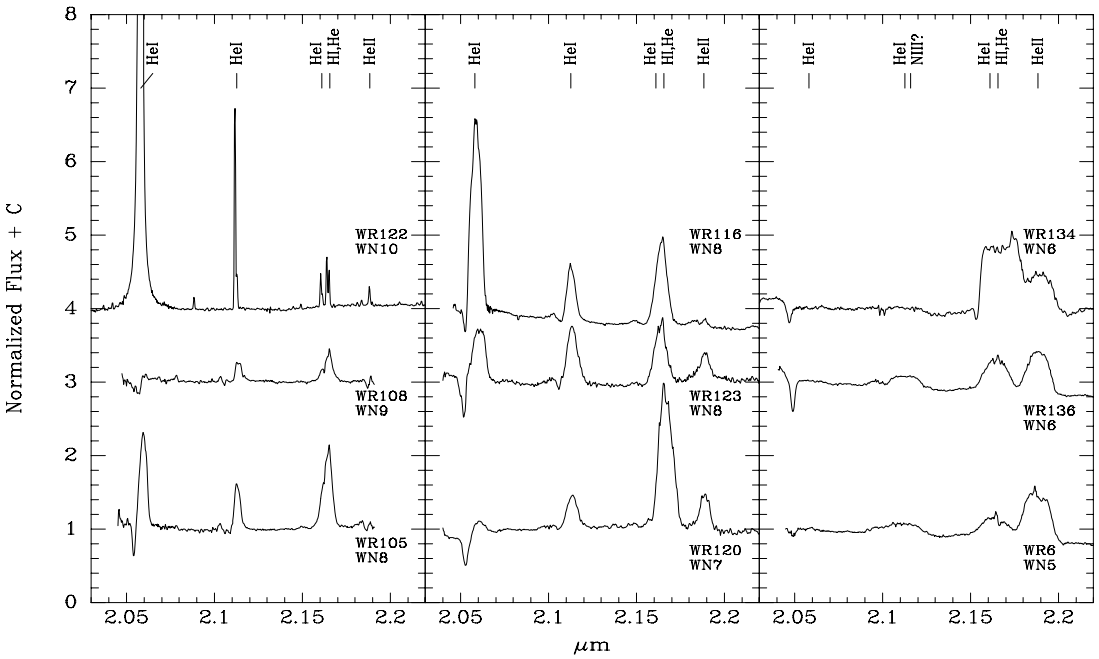

Figure 3.3: Comparison WN Stars. These spectra complement the atlas of NIR spectra of late-WC stars presented by Eenens *et al.* (1991). The 2.058 μm feature in WR122 continues to 33 times the continuum level. Note that apart from WR108 with the controversial classification WN9, there is a readily distinguishable progression with spectral type in the relative strenths of the various He I and then He II features. In particular, the 2.189 μm feature of He II is not prominent in most of the sources later than WN7.

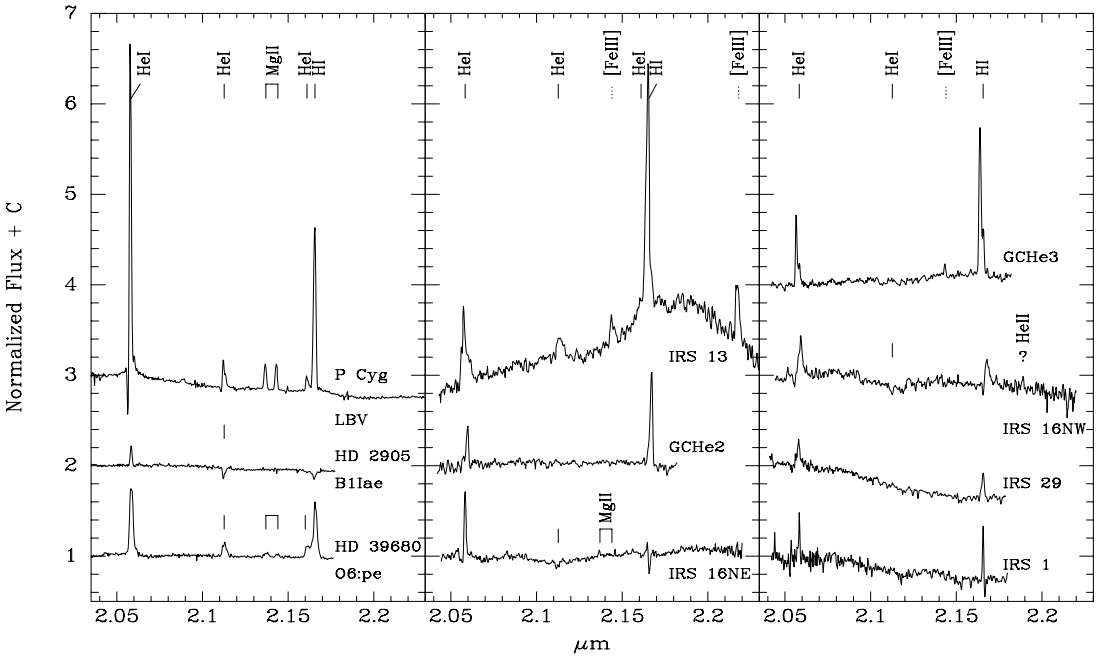

Figure 3.4: Narrow-Lined GC Sources with Selected Comparison Stars. These spectra are distinguishable from the WN classes by their relatively narrow ($< 500\,\mathrm{km/s}$) emission lines. Notable features include the He I 2.112/3 feature in the spectrum of IRS 13 and the Mg II 2.137 and $2.144\,\mu$m features in the spectrum of IRS 16NE. The [Fe III] 2.145 and $2.218\,\mu$m features are nebular. GCHe2, GCHe3, and IRS 29 have not had background correction. The spectra have been normalized to the continuum near $2.06\,\mu$m and shifted.

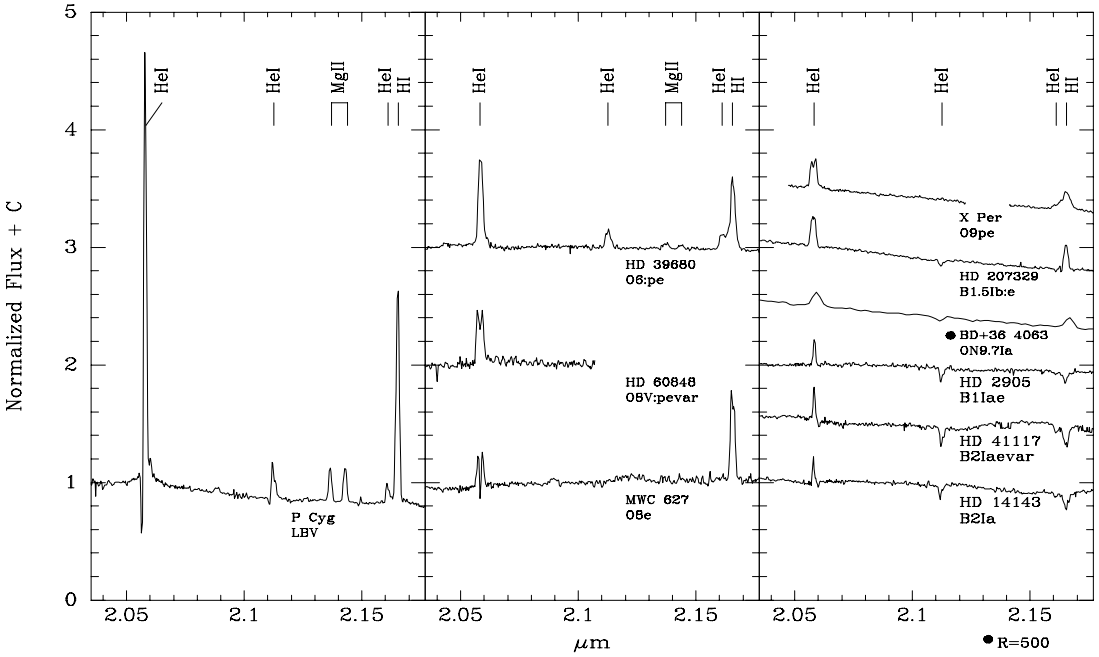

Figure 3.5: Comparison Stars with Significant He I Emission. Only these stars, apart from the WN series, had significant He I 2.058 μm emission. The spectra have been normalized and shifted. The spectrum of BD+36 4063 is relatively low-resolution; the 2.058 μm feature is comparable in strength to the neighboring spectra.